Biomass Conversion and Biorefinery (2022) 12:4171–4181
https://doi.org/10.1007/s13399-022-02558-2

ORIGINAL ARTICLE

Theoretical removal study of gas BTEX onto activated carbon produced from *Digitalis purpurea* L. biomass

Kaan Isinkaralar[1]

Received: 27 January 2022 / Revised: 4 March 2022 / Accepted: 5 March 2022 / Published online: 16 March 2022

Abstract

Exposure to BTEX concentrations may have a remarkable influence on human health because of their existence in indoor air. It is the only solution to remove BTEX from the environment by either ventilation or filtering. Activated carbon is the primary carbon-rich material for the BTEX pollution control strategy. In this study, *Digitalis purpurea* L. biomass as lignocellulosic materials was selected as a common substance in nature and carbonization-appropriate processing. The activated carbons (D_PAC1-60) were prepared from the pyrolysis of *Digitalis purpurea* L. biomass at 500–900 °C by chemical activation with Zinc chloride ($ZnCl_2$), Potassium carbonate (K_2CO_3), Sulfuric acid (H_2SO_4), and Phosphoric acid (H_3PO_4), respectively. The D_PACs structure enrichment was targeted with several conditions (temperature, chemical reagents, etc.). Under the same conditions, the order in which the compared chemicals increased the surface area of D_PACs was as follows $H_3PO_4 > H_2SO_4 > ZnCl_2 > K_2CO_3$. The large surface area was contrived with D_pAC58 (1753.5 m^2/g) at 700 °C by H_3PO_4 activation. The adsorption capacity of BTEX was reached 162 mg/g at 25 °C and 1500 ppm. Consequently, the study revealed that the prepared D_pAC58 from *Digitalis purpurea* L. biomass is suitable for the removal of BTEX from indoor air. The suggestions and prospects for future research were proposed carbon-based materials for indoor air pollutant-removal applications.

Keywords Biomass · Carbonaceous material · Gas phase · Lignocellulosic · VOCs

1 Introduction

In recent years, technological developments in the industry have been rapidly adapted to our current life, including environmental issues [1, 2]. With the usage of advanced industrial products in indoor environments, some air pollutants are formed, the emission of which increases rapidly [3–5]. There are growing concerns about indoor air pollution because people spend more time indoors [6]. They may expose to excessive indoor air pollutants, which have released many sources [7, 8]. One of the most hazardous indoor air pollutants is volatile organic compounds (VOCs) that are threats to human health [9]. Benzene, toluene, ethylbenzene, and xylene, known as BTEX, which evaporate quickly at room temperature (~ 25 °C) from residential indoor environments [10]. The high concentrations of BTEX reveal toxic effects, even carcinogens to humans. Intake of BTEX comes true from computers, photocopiers, cigarette smoke, cooking activities, various chemical-based dyestuffs, some detergents, insecticides, and plastic-based industrial items in indoor air [11–13]. Exposure to high BTEX levels can cause leukemia, aplastic anemia, bone marrow disorders, and some cancers [14]. In the peripheral blood smear test in leukemia patients, exposure to varying concentrations of BTEX shows that there are chromosomal aberrations in lymphocytes and that sister-chromatid exchanges and micronuclei increase the sparseness, and it causes carcinogenicity due to its genotoxic effect [15, 16].

People from many disciplines worldwide are making efforts to improve and enrich indoor air quality. Firstly, it is essential to manage the known sources of indoor air pollutants, freshen the contaminated indoor environment, or remove air pollutants using active or passive air cleaners [17, 18]. Air cleaning systems have been tried to be developed because active air cleaners are not chosen due to their high cost and operational costs. Some indoor cleaning methods, such as biofiltration and adsorption with activated carbon, preferred passive removal systems

✉ Kaan Isinkaralar
kisinkaralar@kastamonu.edu.tr

[1] Department of Environmental Engineering, Faculty of Engineering and Architecture, Kastamonu University, Kastamonu, Türkiye

[19]. The common feature of these systems, which can easily adsorb and reliable technology for volatile organic compounds such as BTEX. Activated carbon has been found in numerous tests to remove BTEX at various levels with high yields [20, 21]. As a result, many materials have been investigated to increase the surface area of activated carbons [22, 23]. It has produced excellent results in BTEX adsorption at various concentrations by highly porous activated carbons, although there is limited research on BTEX removal [24, 25].

Carbonaceous material has been conducted with agricultural waste due to evaluating and recycling waste biomass to the environmental cycle [26, 27]. Studies have been reported that use the lignocellulosic biomass such as *Phragmites australis* [28], *Gossypium malvaceae* [29], *Casuarina equisetifolia* [30], *Artocarpus integer* [31], *Citrus sinnensis* [32], *Hymenaea Courbaril* L. [33], and *Leucaena* [34] for activated carbon and their environmental application [35, 36]. *Digitalis purpurea* L. used in this study is widely distributed, particularly in Anatolia, and all of its components are soft tissue. This plant dies after growing in the nature. Therefore, it cannot be classified as a lignocellulosic waste. The study's main purpose was to investigate usability activated carbon derived from *Digitalis purpurea* L. for adsorption of various concentrations of BTEX. Furthermore, the obtained activated carbon's physicochemical abilities were also characterized and the production conditions. This research was further intended to investigate and compare BTEX molecules on activated carbon under high concentrations.

2 Materials and methods

2.1 Materials

The activated carbon was synthesized by the stem of *Digitalis purpurea* L. (foxglove), and it was collected from nature in Kastamonu, Turkey. Prior to the experiment, it was washed with pure water (Milli Q water, Millipore) several times because it is intended to remove the dust impurities. The lignocellulosic biomass was dried in an oven at 55 °C for 10 days until it gets rid of the moisture content inside and it was sieved to the size range < 500 µm. The powders of the lignocellulosic biomass were put into the oven to dry for the last time at 105 °C. Zinc chloride ($ZnCl_2$, assay 99.5%), potassium carbonate (K_2CO_3, assay 98% +), sulfuric acid (H_2SO_4, 98%), and phosphoric acid (H_3PO_4, 85%) purchased from Merck Millipore Ltd. were applied as the activation agent. BTEX liquid solution (99.5%) was bought from Sigma-Aldrich, USA, and VOC standard solution was taken from Ultra Scientific Inc. All these chemicals were utilized without any further purification in the present study. Samples were weighed by Adam PW 214 brand.

2.2 Production of the activated carbon

Twenty grams of *Digitalis purpurea* L. powders were activated at various impregnation ratios by $ZnCl_2$, K_2CO_3, H_3PO_4, and H_2SO_4, respectively. To assure homogeneity of the mixture (biomass-activating chemicals), they were thoroughly mixed with a manual hand grinder. They were varied from 1:0.5, 1:1, and 1:2 w/w (feedstock ratio/activating agent) for 24 h at ambient temperature. D_pAC was used in the coding of activated carbons. The D_pAC was dried at 105 °C overnight and stored in a desiccator for characterization. The next step was carbonized at 500–900 °C (heating rate was 5 °C/min) for 1.5 h under purified nitrogen gas (N_2 flow rate was 30 mL/min) using high-temperature resistant fixed bed design steel (with 7-cm diameter and 21-cm height.) in a programmable furnace. The produced activated carbon (weight of D_pAC) was washed with 0.3-M HCl solution to remove any remaining chemicals and ash from the carbon structure. Then D_pACs used hot deionized water (80–85 °C) several times until chloride ions were not appointed. The D_pACs were dried at 110 °C for 24 h, and their yield was determined by following Eq. (1).

$$\text{Yield of } D_pAC = (\text{weight of } D_pAC/\text{weight of } \textit{Digitalis purpurea} \text{ L. biomass}) \times 100 \quad (1)$$

2.3 D_pACs characterization

The physicochemical characterization of D_pACs samples was employed to define the surface area and pore size distribution by the adsorption of N_2 at 77 K using Brunauer–Emmett–Teller NOVA 2200e Quantachrome Autosorb surface analyzer (Quantachrome Instruments, Florida, USA). The functional groups on the surface of the D_pACs and their raw material in 400–4000 cm^{-1} were analyzed using PerkinElmer Spectrum 100 Fourier transform infrared (FTIR) (PerkinElmer, Waltham, MA, USA). Thermal degradation of the D_pAC58 and raw material was conducted on the Perkin Elmer Brand Diamond. The morphology of the prepared D_pACs was analyzed by SEM (FEI Quanta FEG 250) and to advance conductivity. All samples were metalized with gold. All analyses are applied to the D_pACs and performed to the raw material. The *Digitalis purpurea* L. biomass was identified by the American Society for Testing and Materials (ASTM) standards E872-82 [37], E871–82

[38], and D1102–84 [39] for volatile matter, moisture, and ash (XRF Xepos II, Spectro). Also, fixed carbon was calculated with Eq. (2).

$$\text{Fixed carbon } \% = 100 - (\text{volatile matter } \% + \text{moisture } \% + \text{ash } \%) \quad (2)$$

Elemental analysis was performed by Euro EA 3000 series, EuroVector, Milano, Italy. Also oxygen content was found from Eq. (3).

$$O\% = 100 - (C\% + H\% + N\% + \text{Moisture}\% + \text{Ash}\%) \quad (3)$$

2.4 Experimental design

The batch reactor for adsorption of BTEX onto the D_pACs was performed with N_2 gas flow (50 mL/min). Also, it formed a vacuum pump (SKC The AirChek XR5000), a gas flow meter, and Tenax TA sorbent tubes used as controls without any contamination. Approximately 0.1 g of D_pACs were placed into the batch reactor at a midpoint of mechanism in Fig. 1.

Firstly, the BTEX solution was prepared and diluted for several initial concentrations (C_o). These experiments were carried out under constant humidity (45-55% RH) and temperature conditions (25°C) using a gravimetric hygrometer (Rotronic, Zurich, Switzerland). The experiments were operated with initial concentrations of 5, 50, 150, 500, 1000–1500 ppm of gas BTEX in times ranging from 0 to 270 min. In this system, in the determination of D_pACs adsorption capacity was investigated the effect of temperatures (carbonization time: 5 °C/min and totally 90 min), activation agents, and impregnation ratios were under inert environment (N_2 flow rate: 100/min), which were tabulated in Table 1.

2.5 Analysis of BTEX

BTEX samples were collected from the batch reactor, which was used 100mg Tenax® TA (60–80 mesh) sampling sorbent tubes and Tenax® TA/Carbotrap/Carboxen 569 (20/45 mesh) by thermal-desorption GC–MS (Agilent 6890 N Network Gas Chromatograph and Agilent 5975 Series also Markes Unity-2 TD), according to EPA Methods, Method TO-17 [40]. The used column was A DB-1 series 123–1063 gas column (Agilent Technologies, Santa Clara, CA, USA). BTEX standard solution (200 µg/mL) purchased from Ultra Scientific brand Aromatic Hydrocarbons Mixture DWM-550–1. The injected sample

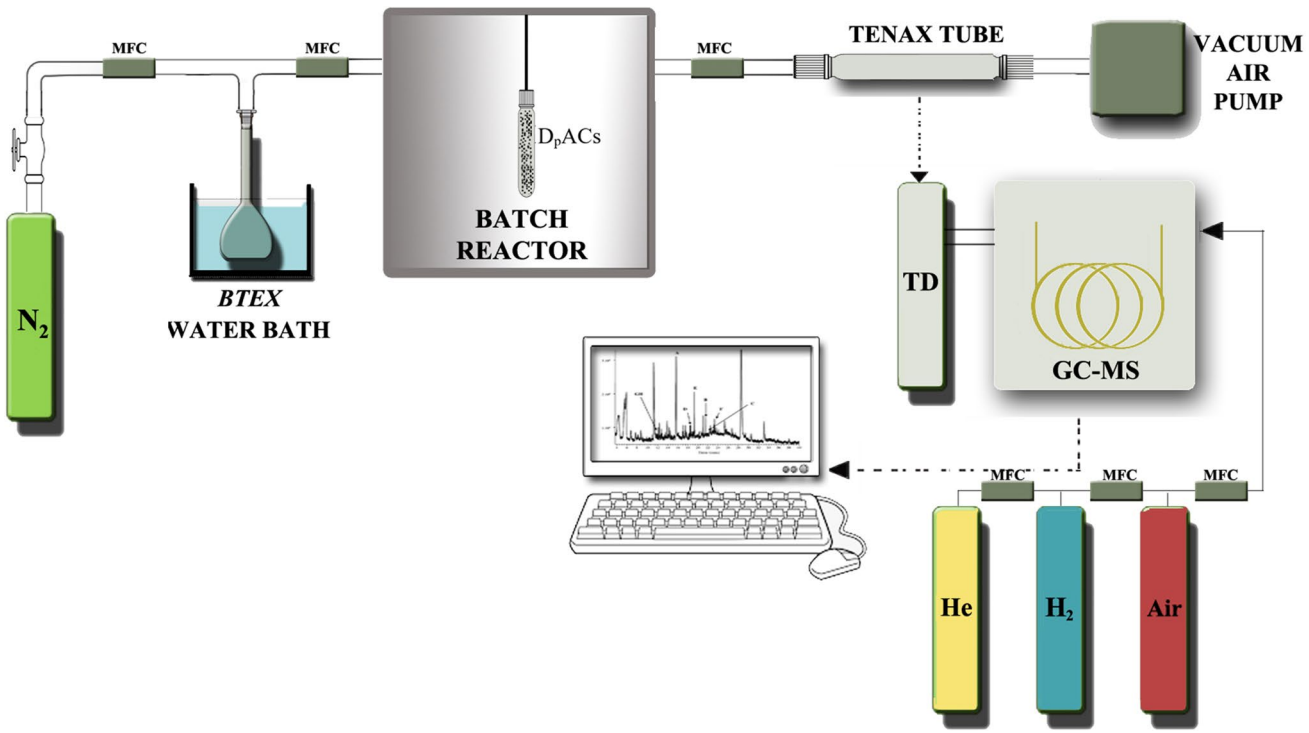

Fig. 1 Experimental design for theoretical removal study of BTEX onto D_pACs

Table 1 The identifications of D_pACs in terms of carbonization and activation process

Activating reagent	Sample ID	Impregnation ratio wt%	Activation temperature °C
$ZnCl_2$	D_pAC1	0.5:1	500
	D_pAC2	0.5:1	600
	D_pAC3	0.5:1	700
	D_pAC4	0.5:1	800
	D_pAC5	0.5:1	900
	D_pAC6	1:1	500
	D_pAC7	1:1	600
	D_pAC8	1:1	700
	D_pAC9	1:1	800
	D_pAC10	1:1	900
	D_pAC11	2:1	500
	D_pAC12	2:1	600
	D_pAC13	2:1	700
	D_pAC14	2:1	800
	D_pAC15	2:1	900
K_2CO_3	D_pAC16	0.5:1	500
	D_pAC17	0.5:1	600
	D_pAC18	0.5:1	700
	D_pAC19	0.5:1	800
	D_pAC20	0.5:1	900
	D_pAC21	1:1	500
	D_pAC22	1:1	600
	D_pAC23	1:1	700
	D_pAC24	1:1	800
	D_pAC25	1:1	900
	D_pAC26	2:1	500
	D_pAC27	2:1	600
	D_pAC28	2:1	700
	D_pAC29	2:1	800
	D_pAC30	2:1	900
H_2SO_4	D_pAC31	0.5:1	500
	D_pAC32	0.5:1	600
	D_pAC33	0.5:1	700
	D_pAC34	0.5:1	800
	D_pAC35	0.5:1	900
	D_pAC36	1:1	500
	D_pAC37	1:1	600
	D_pAC38	1:1	700
	D_pAC39	1:1	800
	D_pAC40	1:1	900
	D_pAC41	2:1	500
	D_pAC42	2:1	600
	D_pAC43	2:1	700
	D_pAC44	2:1	800
	D_pAC45	2:1	900
H_3PO_4	D_pAC46	0.5:1	500
	D_pAC47	0.5:1	600
	D_pAC48	0.5:1	700
	D_pAC49	0.5:1	800
	D_pAC50	0.5:1	900
	D_pAC51	1:1	500
	D_pAC52	1:1	600
	D_pAC53	1:1	700
	D_pAC54	1:1	800
	D_pAC55	1:1	900
	D_pAC56	2:1	500
	D_pAC57	2:1	600
	D_pAC58	2:1	700
	D_pAC59	2:1	800
	D_pAC60	2:1	900

volume was 1 µL, and the detector temperature was 250 °C. Hydrogen gas (40 mL/min) and pure helium gas (20 psi) were used as fuel and carrier gases, respectively. The utilized temperature program began at 35 °C min and then increased to 300 °C with a rate of 5 °C/min for 30 min. Before experiments, all the Tenax tubes were cleaned for 20 min at 330 °C under a nitrogen flow rate of 100 mL/min in a thermal conditioner. The cleaned tubes were closed with brass caps and stored at − 10 °C for a maximum of 2 weeks without any contamination. After that, they were stored at 4 °C for one day then analyzed the day after the BTEX sampling.

2.6 QA and QC of experiments

The reliability of the experiments can be evaluated with quality assurance (QA) and quality control (QC). The QA and QC for adsorption experiments were applied in field blanks and triplicate sample measurements. In the replicate analyses of the reference conditions, discarded limits were found as ± 10.63% for sensibility. They are all repeated until a result was obtained for the empirical blank. Limit of detection (LOD) and limit of quantification (LOQ) were calculated for BTEX concentrations which ranged from 0.00 to 0.41 ppb.

3 Results

3.1 Yield of DpACs

In the production of activated carbon, less loss is desired to get more samples. Therefore, the beginning of the factors affecting the yield, the pyrolysis time, and the applied temperature are directly effective. These effects can keep the high or low yield, ranging from 18.2 to 37.9% after the pyrolysis process as the final product.

3.2 Characterization

The BET surface area and pore structure parameters of the produced activated carbons were carried out by NOVA Touch LX4 nitrogen adsorption–desorption analysis (Quantachrome Instruments, South San Francisco, CA, USA). Also, they were coded D_pAC(1–60), according to the impregnation chemical used $ZnCl_2$, K_2CO_3, H_3PO_4, and H_2SO_4, respectively (Fig. 2). The raw material was determined by the acid detergent fiber (ADF), neutral detergent fiber (NDF), and Klason method [41]. Cellulose, a glucose polymer, 22.5%, hemicellulose 20.8%, another biopolymer consisting of polysaccharide mixtures, lignin, a polymer of phenylpropane monometric units randomly and non-linearly linked by ester bonds, 28.2%, and ash 3.3% were found in Table 2.

According to the International Union of Pure and Applied Chemistry (IUPAC), the adsorption isotherms of D_pAC58 show Type IV isotherm is a typical characteristic of mesoporous materials in the classification of adsorption isotherms [42].

Among the chemicals used, the highest surface area was with H_3PO_4. Therefore, several D_pAC was chosen for high micro and total pore volumes in Table 3. Although D_pAC58 had the highest surface area with 1753.5 m^2/g, the highest micropore volume was found to be 0.388 cm^3/g in D_pAC58.

Figure 3 shows the scanning electron microscopy (SEM) images of *Digitalis purpurea* L. biomass and D_pAC58 as produced activated carbon. The *Digitalis purpurea* L. biomass presents irregular structures and inhomogeneous surfaces with niggardly small cavities while activating with H_3PO_4; it consisted of big cavities with large holes and was observed with relatively higher homogeneity by SEM at a magnification scale of 5000×. The *Digitalis purpurea* L. biomass has a negligible number of pores although D_pAC58 demonstrates pores on its structure due to activating agent H_3PO_4 which helped to release volatile compounds in the raw material. Their surface area was calculated by the BET method [43].

FTIR spectroscopy is used to describe a material's surface functions with functional group between 400 and 4000 cm^{-1}. The *Digitalis purpurea* L. biomass and D_pAC58 were measured absorption spectra and shown in Fig. 4. The band at 3568 cm^{-1} comes across to O–H

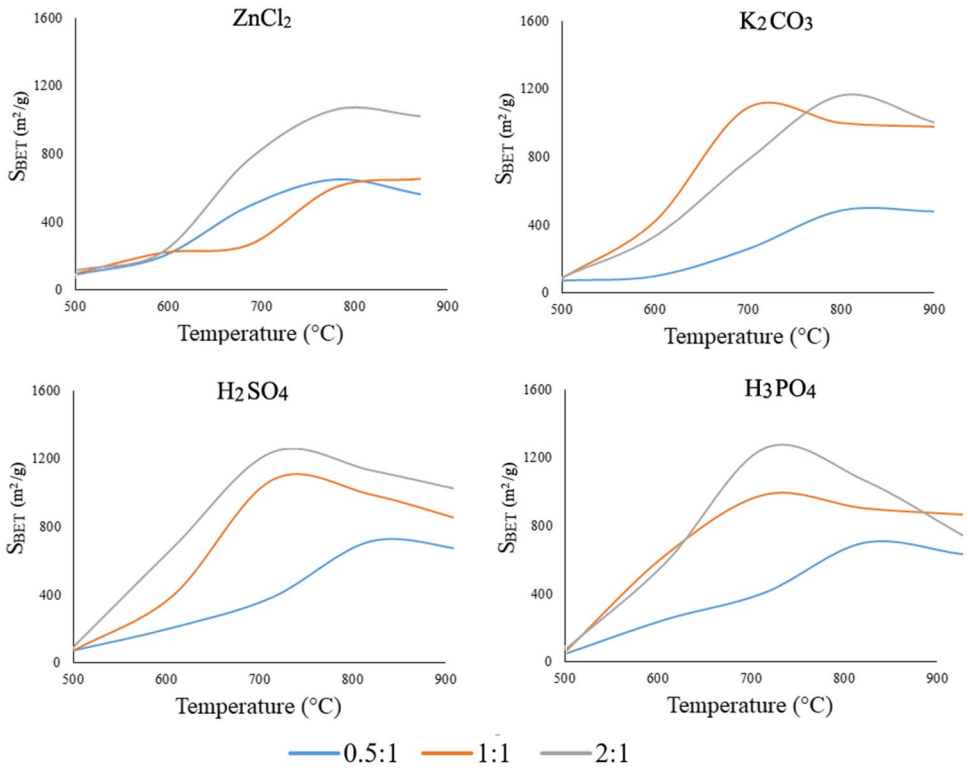

Fig. 2 S_{BET} values of D_pACs samples at different carbonization temperatures and using activating agents

Table 2 The contents of *Digitalis purpurea* L. biomass

Cellulose wt%	Hemicellulose wt%	Lignin wt%	Ash %	Moisture %	Volatile matter %	Fix C %	C %	H %	N %	O %
22.5	20.8	28.2	3.3	10.1	72.9	13.71	45.3	6.2	1.3	33.8

stretching hydroxyl groups in the *Digitalis purpurea* L. biomass structure (lignin, cellulose, and hemicellulose structures) available in alcohol and acids [44]. The band located at 2978 cm^{-1} is bound to sp2 C–H and sp^3 C–H stretching [45]. The peak at 1422 cm^{-1} is connected to the alkanes and alkyls. The bands at 1056 and 1000 are in a combination with C–O stretching of hydroxyls in the structure of cellulose and hemicellulose [46]. The bands between 900 cm^{-1} and 700 cm^{-} are aromatic C–H stretching inorganic forms. Compared with raw material and D_pAC58, the *Digitalis purpurea* L. biomass has more absorption peaks. However, D_pAC58 has fewer peaks because chemically activated with H_3PO_4 and has annihilated most of the organic structure from the lignocellulosic raw material.

The thermogravimetric (TGA) curves of the *Digitalis purpurea* L. biomass and D_pAC58 were acquired in 25 °C – 800 °C with a heating rate of 10 °C min^{-1}. They were heated as a solid mass of 7 mg under the gas flow of N_2. Figure 5 shows the thermal stability of samples, in which three main stages was seen in both samples. The *Digitalis purpurea* L. biomass exhibited that first stage which occurred between 40 and 185 °C with 8.96 wt% loss. The second stage presented between 185 and 370 °C with 22.18 wt% loss, and the third stage from 370 to 800 °C with 19.22 wt% loss. Decomposition of organic volatiles was observed in the steps with rapid loss and lignin decomposition in the other steps [47]. The first stage of D_pAC58 was monitored between 35 and 165 °C with 17.65 wt% loss. The second stage was seen between 165 and 570 °C with 14.33 wt% loss, and the final stage was gained between 570 and 780 °C with 8.64 wt% loss which took place. The D_pAC58 was showed excellent adsorptive properties due to its micro-porous structure [48].

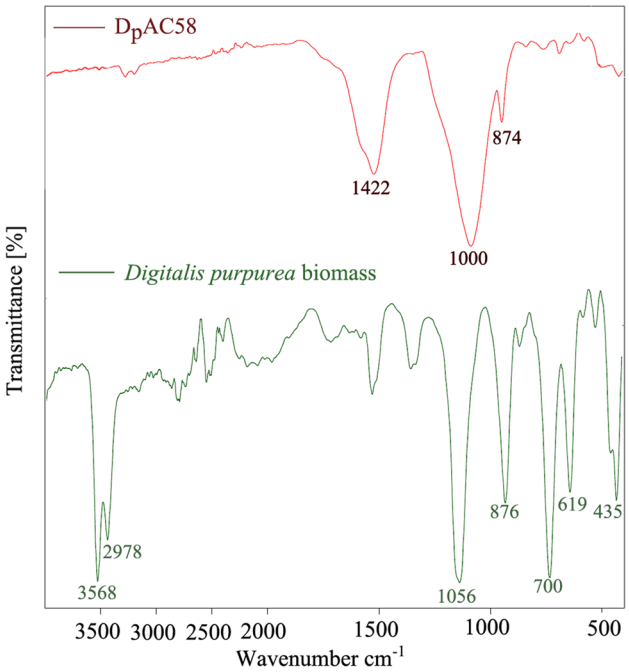

Fig. 4 FTIR spectrum of the *Digitalis purpurea* L. biomass and D_pAC58

Table 3 The pore structures of D_pACs

Samples	S_{BET} (m^2/g)	V_{micro} (cm^3/g)	V_{total} (cm^3/g)
D_pAC14	1005.2	0.137	0.238
D_pAC43	1521.7	0.241	0.382
D_pAC44	1387.4	0.234	0.377
D_pAC58	1753.5	0.388	0.497
D_pAC59	1487.3	0.311	0.399

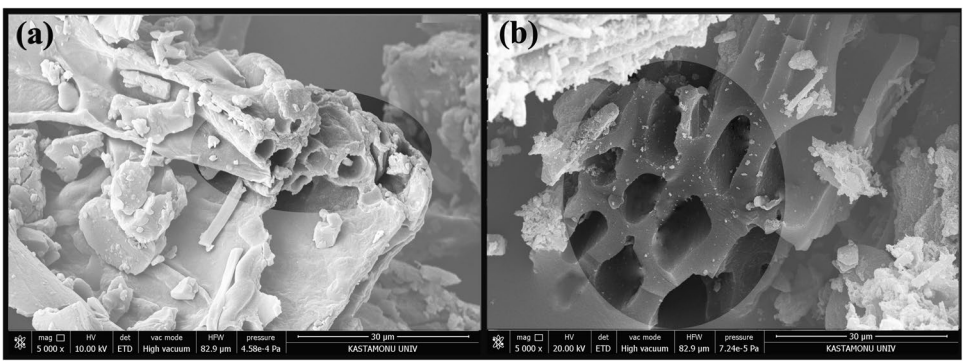

Fig. 3 SEM micrographs at 30 µm (**a**: *Digitalis purpurea* L. biomass, **b**: D_pAC58)

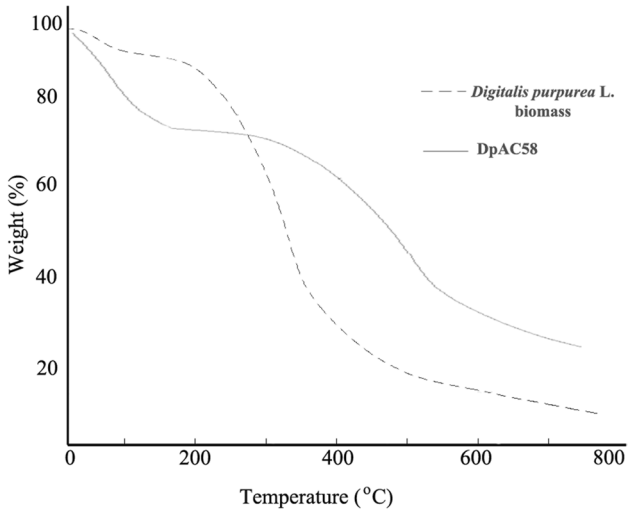

Fig. 5 TGA curves of the *Digitalis purpurea* L. biomass and D_pAC58

3.3 Adsorption of gas-phase BTEX

For the steady-state conditions, the experimental setup was carried out without adsorbate, including gas-phase BTEX into the system due to the detecting of the BTEX gas adhering to the wall. The efficiency of adsorbents varies depending on initial concentration and contact time. The adsorption capacity of an adsorbent is the milligrams of adsorbate per 1 g of D_pACs. The highest surface area was obtained with H_3PO_4. Therefore, D_pAC14, D_pAC44, D_pAC58, and D_pAC59 were used in BTEX removal experiments. Before starting the investigation, it waited for about 30 minutes to stabilize for each experiment.

3.3.1 Initial concentration

The experimental study performed different initial BTEX concentrations which ranged from 5 to 1500 ppm. While the lowest value studied was 35.6 mg/g at 5 ppm, 162 mg/g was obtained at 1500 ppm. As the concentration amount increases, the filling of the pores of the activated carbon increases in Fig. 6.

The stabile in removing the amount adsorbed was found when the initial concentration increased to 500 ppm. In this context, a high amount of adsorbed is found with high concentration because the pores are sufficiently filled.

3.3.2 Contact time

The effect of contact time on the BTEX adsorption study was examined until 300 min. After that, each measurement was made at 30-min intervals. The removal efficiency of BTEX was shown that rise slope in 90 min, then increase slowly until 210 min, and finally, the saturation point was reached at 270 min in Fig. 7.

The movement of BTEX molecules first became fast and then slow. Adhering molecules caused the pores to fill rapidly and then the rate of attachment to slow down. The adsorbate speed before the pores are filled, and the bond speed of BTEX molecules after they are filled affects the adsorption capacity. As the pores fill, the BTEX molecules need more time. The maximum BTEX concentration was 1500 ppm and reached 270 min at a saturation level of 162 mg/g.

4 Discussion

The D_pACs were performed and compared with several initial concentrations which ranged from 5 to 1500 ppm at 25 °C. The maximum adsorption capacity values were obtained from synthesized with H_3PO_4-activated carbons. Although the BET surface area of D_pAC58 is large, it has been observed that the micropore volume is more prominent in D_pAC59. Hence, the holding capacity of BTEX molecules is higher in the experiments. D_pACs

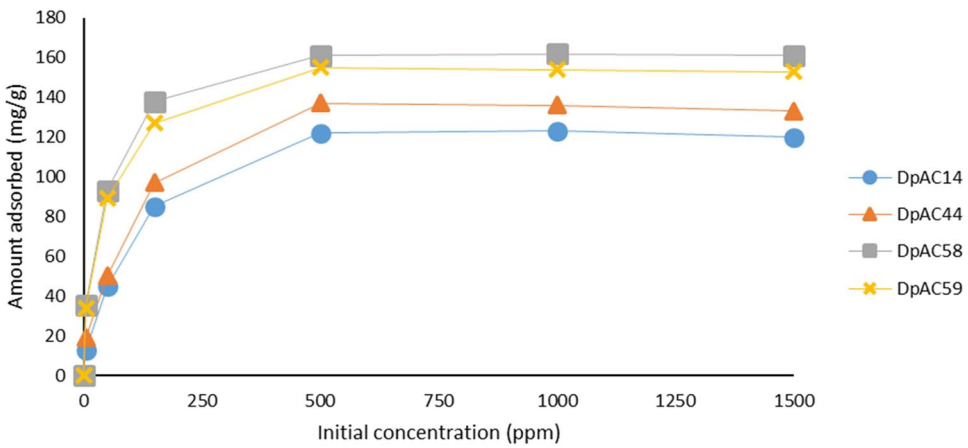

Fig. 6 Effect of initial concentration and amount of adsorbed BTEX

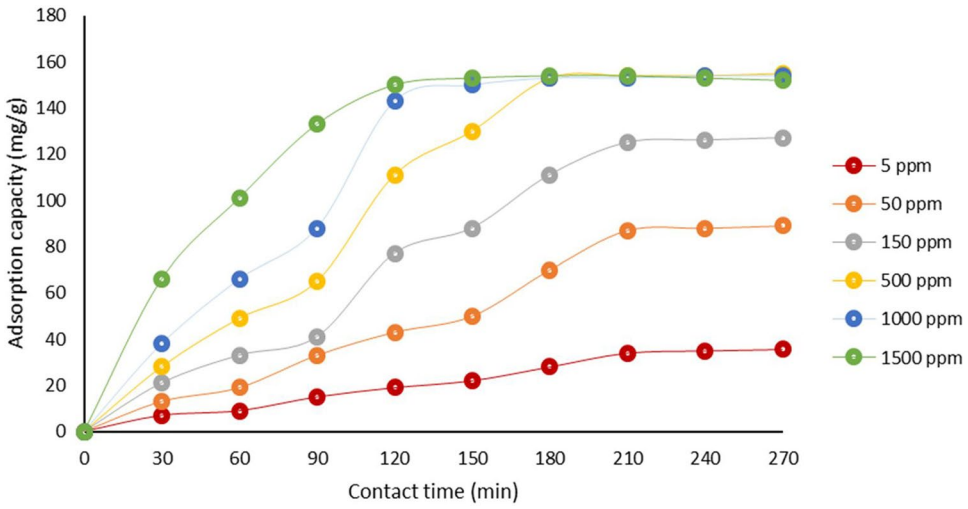

Fig. 7 Variation of BTEX adsorption capacity and contact time

compared to studies in the literature show that the surface area seems fine for a lignocellulosic-based activated carbon by Nor et al. [49]. Despite the removal of BTEX gases in the aquatic environment with activated carbon, it is seen that the number of studies on the reduction of BTEX in the gas phase with activated carbon is quite limited. Especially at the same time, it is difficult to remove these simultaneous gases. Nam et al. [50] experimented on the TMA and H_2S gas purification with activated carbon from rice husk as a biomass waste. Using KOH, they performed carbonization in a fixed bed reactor using argon (inert environment). Also, they investigated adsorption isotherms, including Langmuir and Freundlich, and adsorbents found as effective for TMA and H_2S gas removal. Wang and Sheng [51] revealed that gas-toluene (initial toluene concentration: 1–10 ppm) adsorption with activated carbon for gas–solid mass transfer and its behavior. They used a model that Grand Canonical Monte Carlo (GCMC) explained the toluene adsorption process with molecules. Liu et al. [52] were derived from bamboo (Anhui, China) by chemical activation using KOH/CB of 4:1. ACB-1 maximum surface area found 2133.2 m^2/g and pore volume of 0.94 cm^3/g. They tried the adsorption of dye from RhB solution and reached adsorption capability as > 1200 mg/g. Saha et al. [53] produced powdered activated carbon (PAC has 2250 m^2/g, total pore volume 1.1 cm^3/g) and investigated BTX (benzene, toluene, xylene) adsorption. Initial BTX concentrations were 100 ppm, and 0.025 g activated carbon for each solution, and adsorption capacity was determined at 600 mg/g. Kang et al. [54] have experimented with solid waste from biomass for activated carbon production via the chemical (H_3PO_4) method. The samples were analyzed by SEM, FT-IR, XRD, BET, and TG for texture characteristics. Adsorption of methylene blue was performed with AC400 and found 1125 mg/g. Oh et al. [55] used RAC-2 and commercial activated carbon from coconut shells (CAC). RAC-2 (1286 m^2/g) and CAC (1153 m^2/g) had almost similar surface areas and tried for the removal of VOCs. They searched performance of them under humidity conditions and that the capacity decreased benzene adsorption with the increase in humidity. Isinkaralar et al. [56] investigated gas-phase BTEX removal with activated carbon (AC-KN) from *Aesculus hippocastanum* L. biomass by $ZnCl_2$. The AC-KN was eliminated BTEX range simultaneously from 638 to 1114 µg/g for several concentrations.

In some studies, HEPA filters have been tried instead of activated carbon-based filters. However, the efficiency of VOC retention of HEPA filters is very low and difficult to clean, according to Chen et al. [57]. Therefore, they may not be used only but need to be added with activated carbon as a supplement. Zhang et al. [58] synthesized three different MOF adsorbents and HEPA, which were evaluated simultaneously with $PM_{2.5}$ and toluene. The MOF was found to better perform for toluene removal. In addition, the carbon and lignin contents of the lignocellulosic biomass used were effective. Generally, adsorption was effective method on different molecular sizes and affinities for pollutants and volatile organic compounds [59, 60]. All these removal studies were carried out through a reactor and that the level and duration of BTEX have been adapted to indoor conditions (high or low). Also, simultaneous removal of multi-air-pollutant is a crucial issue with other VOCs in the real indoor environment [61].

5 Conclusion

In summary, activated carbon from the *Digitalis purpurea* L. biomass was successfully prepared for the effective and economical removal of BTEX from indoor air by chemical

method. As an adsorbent, D_pAC58 is a talented low-cost and eco-friendly carbonaceous material for annihilating BTEX from indoor air. The characterization of D_pAC58 results shows that they were well done synthesized with similar morphology (SEM, BET, FT-IR). The carbonization of its biomass occurs in well-developed pores on the surface morphology. Therefore, it seems more appropriate to investigate optimum conditions with dwell time and activation agents. The effective removal of BTEX is the most important indoor air quality management issue due to posing a severe threat to human health. The highest concentration of the BTEX adsorption process reached equilibrium within 150 min of contact time at room temperature. The D_pAC58 was used as critical sorbents for BTEX removal from indoor air. The superiority of D_pAC58 is inexpensive and has a high holding capability to remove BTEX from indoor air. However, future studies could explore investigating the removal of other indoor air pollutants with real field applications.

Data availability The data that support the findings of this study are available from the corresponding author, upon reasonable request.

Declarations

Ethics approval Not applicable

Conflict of interest The author declares no competing interests.

References

1. Irga PJ, Pettit TJ, Torpy FR (2018) The phytoremediation of indoor air pollution: a review on the technology development from the potted plant through to functional green wall biofilters. Reviews in Environmental Science and Bio/Technology 17(2):395–415. https://doi.org/10.1007/s11157-018-9465-2
2. Yilmaz D, Isinkaralar O (2021) How can natural environment scoring tool (Nest) be adapted for urban parks?. Kastamonu University Journal of Engineering and Sciences, 7(2), 127–139. https://dergipark.org.tr/en/pub/kastamonujes/issue/66389/1013821
3. Phongphetkul P, Mangkang S, Praditsmanont A, Intrachooto S, Choruengwiwat J, Treesubsuntorn C, Thiravetyan P (2021) Evaluation of indoor air quality in high-rise residential buildings in Bangkok and factor analysis. Environ Monit Assess 193(1):1–11. https://doi.org/10.1007/s10661-020-08792-3
4. Varol T, Cetin M, Ozel HB, Sevik H, Zeren Cetin I (2022) The effects of climate change scenarios on Carpinus betulus and Carpinus orientalis in Europe. Water Air Soil Pollut 233(2):1–13. https://doi.org/10.1007/s11270-022-05516-w
5. Yilmaz D, Isinkaralar O (2021) Climate action plans under climate-resilient urban policies. Kastamonu University Journal of Engineering and Sciences, 7(2), 140–147. https://dergipark.org.tr/en/pub/kastamonujes/issue/66389/1014599
6. Sevik H, Isinkaralar K, Isinkaralar O (2018) Indoor air quality in hospitals: the case of Kastamonu Turkey. J Chem Biol Phys Sci Sect D 9(1):67–73
7. Cancelada L, Sleiman M, Tang X, Russell ML, Montesinos VN, Litter MI, Gundel LA, Destaillats H (2019) Heated tobacco products: volatile emissions and their predicted impact on indoor air quality. Environ Sci Technol 53(13):7866–7876. https://doi.org/10.1021/acs.est.9b02544
8. Elsunousi AAM, Sevik H, Cetin M, Ozel HB, Ozel HU (2021) Periodical and regional change of particulate matter and CO_2 concentration in Misurata. Environ Monit Assess 193:707. https://doi.org/10.1007/s10661-021-09478-0
9. Pitarma R, Marques G, Ferreira BR (2017) Monitoring indoor air quality for enhanced occupational health. J Med Syst 41(2):1–8. https://doi.org/10.1007/s10916-016-0667-2
10. Rao PS, Ansari MF, Gavane AG, Pandit VI, Nema P, Devotta S (2007) Seasonal variation of toxic benzene emissions in petroleum refinery. Environ Monit Assess 128(1):323–328. https://doi.org/10.1007/s10661-006-9315-5
11. Chen R, Li T, Huang C, Yu Y, Zhou L, Hu G, Yang F, Zhang L (2021) Characteristics and health risks of benzene series and halocarbons near a typical chemical industrial park. Environ Pollut 289:117893. https://doi.org/10.1016/j.envpol.2021.117893
12. Zhu J, Zhao X, Yang M, Zheng B, Sun C, Zou X, Liu Z, Harada KH (2021) Levels of urinary metabolites of benzene compounds, trichloroethylene, and polycyclic aromatic hydrocarbons and their correlations with socioeconomic, demographic, dietary factors among pregnant women in six cities of China. Environmental Science and Pollution Research, 1–16. https://doi.org/10.1007/s11356-021-16030-7. https://doi.org/10.1166/asl.2017.8267
13. Ghoma WEO, Sevik H, Isinkaralar K (2022) Using indoor plants as biomonitors for detection of toxic metals by tobacco smoke. Air Quality, Atmosphere & Health, 1-10. https://doi.org/10.1007/s11869-021-01146-z
14. Goldstein BD (2010) Benzene as a cause of lymphoproliferative disorders. Chem Biol Interact 184(1–2):147–150. https://doi.org/10.1016/j.cbi.2009.12.021
15. Cox Jr LA (2021) Case study: are low concentrations of benzene disproportionately dangerous?. In Quantitative risk analysis of air pollution health effects (pp. 325–353). Springer, Cham. DOI: https://doi.org/10.1007/978-3-030-57358-4_12
16. Tabatabaei Z, Baghapour MA, Hoseini M, Fararouei M, Abbasi F, Baghapour M (2021) Assessing BTEX concentrations emitted by hookah smoke in indoor air of residential buildings: health risk assessment for children. J Environ Health Sci Eng 19(2):1653–1665. https://doi.org/10.1007/s40201-021-00721-x
17. Gonçalves AD, Martins TG, Cassella RJ (2021) Passive sampling of toluene (and benzene) in indoor air using a semipermeable membrane device. Ecotoxicol Environ Saf 208:111707. https://doi.org/10.1016/j.ecoenv.2020.111707
18. Wargocki P, Wei W, Bendžalová J, Espigares-Correa C, Gerard C, Greslou O, Rivallain M, Sesana MM, Olesen WB, Zirngibl J, Mandin C (2021) TAIL, a new scheme for rating indoor environmental quality in offices and hotels undergoing deep energy renovation (EU ALDREN project). Energy and Buildings 244:111029. https://doi.org/10.1016/j.enbuild.2021.111029
19. Bakar NA, Othman N, Yunus ZM, Altowayti WA H, Al-Gheethi A, Asharuddin SM, Tahir M, Fitriani N, Mohd-Salleh SNA (2021) Nipah (Musa Acuminata Balbisiana) banana peel as a lignocellulosic precursor for activated carbon: characterization study after carbonization process with phosphoric acid impregnated activated carbon. Biomass Conversion and Biorefinery, 1-14. https://doi.org/10.1007/s13399-021-01937-5
20. Shoaib AG, El-Sikaily A, El Nemr A, Mohamed AEDA, Hassan AA (2020) Testing the carbonization condition for high surface area preparation of activated carbon following type IV green alga Ulva lactuca. Biomass Conversion and Biorefinery, 1-16. https://doi.org/10.1007/s13399-020-00823-w

21. Jahan K, Singh V, Mehrotra N, Rathore K, Verma V (2021) Development of activated carbon from KOH activation of pre-carbonized chickpea peel residue and its performance for removal of synthetic dye from drinking water. Biomass Conversion and Biorefinery, 1-11. https://doi.org/10.1007/s13399-021-01938-4
22. Adan-Mas A, Alcaraz L, Arévalo-Cid P, López-Gómez FA, Montemor F (2021) Coffee-derived activated carbon from second biowaste for supercapacitor applications. Waste Manage 120:280–289. https://doi.org/10.1016/j.wasman.2020.11.043
23. Medhat A, El-Maghrabi HH, Abdelghany A, Menem NMA, Raynaud P, Moustafa YM, Elsayed AM, Nada AA (2021) Efficiently activated carbons from corn cob for methylene blue adsorption. Applied Surface Science Advances 3:100037. https://doi.org/10.1016/j.apsadv.2020.100037
24. Gao J, Qi X, Zhang D, Matsuoka T, Nakamura Y (2021) Propagation of glowing combustion front in a packed bed of activated carbon particles and the role of CO oxidation. Proc Combust Inst 38(3):5023–5032. https://doi.org/10.1016/j.proci.2020.05.041
25. Naciri Y, Hsini A, Bouziani A, Djellabi R, Ajmal Z, Laabd M, Navio AJ, Mills A, Bianchi LC, Li H, Bakiz B, Albourine A (2021) Photocatalytic oxidation of pollutants in gas-phase via Ag3PO4-based semiconductor photocatalysts: recent progress, new trends, and future perspectives. Critical Reviews in Environmental Science and Technology, 1-44. https://doi.org/10.1080/10643389.2021.1877977
26. MacDermid-Watts K, Pradhan R, Dutta A (2021) Catalytic hydrothermal carbonization treatment of biomass for enhanced activated carbon: a review. Waste and Biomass Valorization 12(5):2171–2186. https://doi.org/10.1007/s12649-020-01134-x
27. Guo Z, Zhang X, Kang Y, Zhang J (2017) Biomass-derived carbon sorbents for Cd (II) removal: activation and adsorption mechanism. ACS Sustainable Chemistry & Engineering 5(5):4103–4109. https://doi.org/10.1021/acssuschemeng.7b00061
28. Sartova K, Omurzak E, Kambarova G, Dzhumaev I, Borkoev B, Abdullaeva Z (2019) Activated carbon obtained from the cotton processing wastes. Diam Relat Mater 91:90–97. https://doi.org/10.1016/j.diamond.2018.11.011
29. Ravichandran P, Sugumaran P, Seshadri S, Basta AH (2018) Optimizing the route for production of activated carbon from Casuarina equisetifolia fruit waste. Royal Society open science 5(7):171578. https://doi.org/10.1098/rsos.171578
30. Selvaraju G, Bakar NKA (2017) Production of a new industrially viable green-activated carbon from Artocarpus integer fruit processing waste and evaluation of its chemical, morphological and adsorption properties. J Clean Prod 141:989–999. https://doi.org/10.1016/j.jclepro.2016.09.056
31. Tovar AK, Godínez LA, Espejel F, Ramírez-Zamora RM, Robles I (2019) Optimization of the integral valorization process for orange peel waste using a design of experiments approach: production of high-quality pectin and activated carbon. Waste Manage 85:202–213. https://doi.org/10.1016/j.wasman.2018.12.029
32. Spessato L, Bedin KC, Cazetta AL, Souza IP, Duarte VA, Crespo LH, Silva MC, Pontes RM, Almeida VC (2019) KOH-super activated carbon from biomass waste: insights into the paracetamol adsorption mechanism and thermal regeneration cycles. J Hazard Mater 371:499–505. https://doi.org/10.1016/j.jhazmat.2019.02.102
33. Abdel-Galil EA, Rizk HE, Mostafa AZ (2016) Production and characterization of activated carbon from Leucaena plant wastes for removal of some toxic metal ions from waste solutions. Desalin Water Treat 57(38):17880–17891. https://doi.org/10.1080/19443994.2015.1102768
34. Isinkaralar K, Erdem R (2021) Landscape plants as biomonitors for magnesium concentration in some species. International Journal of Progressive Sciences and Technologies 29(2):468–473
35. Isinkaralar K, Erdem R (2022) The effect of atmospheric deposition on potassium accumulation in several tree species as a biomonitor. Environmental Research and Technology, 5(1), https://doi.org/10.35208/ert.1026602
36. ASTM International (2019) E872–82 Standard test method for volatile matter in the analysis of particulate wood fuels. Am Soc Mater Test Int. https://doi.org/10.1520/E0872-82R19
37. ASTM International (2019) E871–82 Standard test method for moisture analysis of particulate wood fuels. Am Soc Mater Test Int. https://doi.org/10.1520/E0871-82R19
38. ASTM International (2021) D1102–84 Standard test method for ash in wood. Am Soc Mater Test Int. https://doi.org/10.1520/D1102-84R21
39. US EPA (1999) Determination of volatile organic compounds in ambient air using active sampling onto sorbent tubes, Compendium of methods for the determination of toxic organic compounds in ambient air, Second Edition Compendium Method TO-17, U.S. Environmental Protection Agency (US EPA), Washington, DC.
40. Hoareau W, Trindade WG, Siegmund B, Castellan A, Frollini E (2004) Sugar cane bagasse and curaua lignins oxidized by chlorine dioxide and reacted with furfuryl alcohol: characterization and stability. Polym Degrad Stab 86(3):567–576. https://doi.org/10.1016/j.polymdegradstab.2004.07.005
41. Thommes M, Kaneko K, Neimark AV, Olivier JP, Rodriguez-Reinoso F, Rouquerol J, Sing KSW (2015) Physisorption of gases, with special reference to the evaluation of surface area and pore size distribution (IUPAC Technical Report). Pure Appl Chem 87(9–10):1051–1069
42. Sing KS (2004) Characterization of porous materials: past, present and future. Colloids Surf, A 241(1–3):3–7. https://doi.org/10.1016/j.colsurfa.2004.04.003
43. Biswas B, Pandey N, Bisht Y, Singh R, Kumar J, Bhaskar T (2017) Pyrolysis of agricultural biomass residues: comparative study of corn cob, wheat straw, rice straw and rice husk. Biores Technol 237:57–63
44. Zawawi NM, Hamzah F, Nasarudin NA, Azman NN (2017) Comparison on the properties of activated carbon derived from rubber seed shell and bamboo. Adv Sci Lett 23:3921–3925
45. Ismail IS, Rashidi NA, Yusup S (2021) Production and characterization of bamboo-based activated carbon through single-step H_3PO_4 activation for CO_2 capture. Environmental Science and Pollution Research, 1-7. https://doi.org/10.1007/s11356-021-15030-x
46. Elaigwu SE, Greenway GM (2019) Characterization of energy-rich hydrochars from microwave-assisted hydrothermal carbonization of coconut shell. Waste and Biomass Valorization 10(7):1979–1987. https://doi.org/10.1007/s12649-018-0209-x
47. Saber SEM, Abd Rahim SB, Yussof HW, Olalere OA, Habeeb OA (2019) Morphological, thermal stability and textural elucidation of raw and activated palm kernel shell and their potential use as environmental-friendly adsorbent. Chemical Data Collections 21:100235. https://doi.org/10.1016/j.cdc.2019.100235
48. Nor NM, Lau LC, Lee LC, Teong K, Mohamed AR (2013) Synthesis of activated carbon from lignocellulosic biomass and its applications in air pollution control—a review. J Environ Chem Eng 1(4):658–666. https://doi.org/10.1016/j.jece.2013.09.017
49. Nam H, Wang S, Jeong HR (2018) TMA and H_2S gas removals using metal loaded on rice husk activated carbon for indoor air purification. Fuel 213:186–194. https://doi.org/10.1016/j.fuel.2017.10.089
50. Wang M, Sheng Y (2022) Molecular simulation to analyze the influence of ultrafine particles on activated carbon adsorbing low concentration toluene. Building and Environment, 108875. https://doi.org/10.1016/j.buildenv.2022.108875

51. Liu H, Xu C, Wei X, Ren Y, Tang D, Zhang C, Zhang R, Li F, Huo C (2020) 3D hierarchical porous activated carbon derived from bamboo and its application for textile dye removal: kinetics, isotherms, and thermodynamic studies. Water Air Soil Pollut 231(10):1–18. https://doi.org/10.1007/s11270-020-04883-6
52. Saha D, Mirando N, Levchenko A (2018) Liquid and vapor phase adsorption of BTX in lignin derived activated carbon: equilibrium and kinetics study. J Clean Prod 182:372–378. https://doi.org/10.1016/j.jclepro.2018.02.076
53. Kang S, Jiang S, Peng Z, Lu Y, Guo J, Li J, Zeng W, Lin X (2018) Valorization of humins by phosphoric acid activation for activated carbon production. Biomass conversion and biorefinery 8(4):889–897. https://doi.org/10.1007/s13399-018-0329-3
54. Oh JY, You YW, Park J, Hong JS, Heo I, Lee CH, Suh JK (2019) Adsorption characteristics of benzene on resin-based activated carbon under humid conditions. J Ind Eng Chem 71:242–249. https://doi.org/10.1016/j.jiec.2018.11.032
55. Isinkaralar K, Gullu G, Turkyilmaz A (2022) Experimental study of formaldehyde and BTEX adsorption onto activated carbon from lignocellulosic biomass. Biomass Conversion and Biorefinery, 1-11. https://doi.org/10.1007/s13399-021-02287-y
56. Chen R, Shiue A, Liu J, Zhi, Y, Zhang D, Xia F, Leggett G (2022) Integrated on-site collection and off-site analysis of airborne molecular contamination in cleanrooms for integrated circuit manufacturing processes. Building and Environment, 108941. https://doi.org/10.1016/j.buildenv.2022.108941
57. Zhang X, Li Y, Zhang Z, Nie M, Wang L, Zhang H (2021) Adsorption of condensable particulate matter from coal-fired flue gas by activated carbon. Sci Total Environ 778:146245. https://doi.org/10.1016/j.scitotenv.2021.146245
58. Doğan M, Alkan M, Türkyilmaz A, Özdemir Y (2004) Kinetics and mechanism of removal of methylene blue by adsorption onto perlite. J Hazard Mater 109(1–3):141–148. https://doi.org/10.1016/j.jhazmat.2004.03.003
59. Turan Beyli P, Doğan M, Alkan M, Türkyılmaz A, Turhan Y, Demirbaş Ö, Namli H (2016) Characterization, adsorption, and electrokinetic properties of modified sepiolite. Desalin Water Treat 57(41):19248–19261. https://doi.org/10.1080/19443994.2015.1102773
60. Wang H, Yuan B, Hao R, Zhao Y, Wang X (2019) A critical review on the method of simultaneous removal of multi-air-pollutant in flue gas. Chem Eng J 378:122155. https://doi.org/10.1016/j.cej.2019.122155